
Data-Driven Generalized Integer Aperture Bootstrapping for High-Integrity Positioning

G. Nathan Green, *The University of Texas at Austin*
Dr. Todd Humphreys, *The University of Texas at Austin*

Abstract—A new method is developed for integer ambiguity resolution in carrier-phase differential global navigation satellite system (CDGNSS) positioning. The method is novel in that it is simultaneously (1) data-driven, (2) generalized to include partial ambiguity resolution, and (3) amenable to a full analytical characterization of the prior probabilities of correctly- and incorrectly-resolved ambiguities. The technique is termed generalized integer aperture bootstrapping, or GIAB. A full development of GIAB is provided herein, including sizing its integer aperture to usually produce a higher prior probability of full ambiguity resolution than comparable existing methods. In Monte-Carlo simulations, GIAB is shown to provide nearly optimal ambiguity resolution success rates of full ambiguity resolution for relevant integrity requirements under strong models while enabling partial ambiguity resolution.

Keywords—Generalized integer aperture, bootstrap, CDGNSS, integrity, availability, partial ambiguity resolution, LAMBDA, data-driven

I. INTRODUCTION

The next generation of CDGNSS use cases includes fully autonomous landing and refueling of large, unmanned aerial vehicles, and automated land vehicle navigation. These applications will demand decimeter-level position accuracy and more stringent solution integrity than all previous applications. Integrity is specified in terms of integrity risk (IR), the probability that the solution error exceeds an alert limit (AL) without warning. The percentage of time that a system meets its required navigation performance, including accuracy and IR , is called solution availability. For safety-of-life applications, IR is on the order of 10^{-7} per hour, with required availability in excess of 99% [1].

This paper focuses on the portion of the IR budget allocated to incorrect resolution, or fixing, of the carrier-phase integer ambiguities that are a central feature of CDGNSS positioning. This portion is specified as the acceptable probability of incorrect fix, or failure rate, \bar{P}_F . High-integrity CDGNSS techniques must provably satisfy demandingly low \bar{P}_F . Two such methods are the Geometry Extra Redundant Almost Fixed Solutions (GERAFS) [2] and the Enforced Position-domain Integrity-risk of Cycle resolution (EPIC) [3]–[6] algorithms. Both of these rely exclusively on *a priori* error models to determine, before the measurements are processed, whether a fixed solution or a float backup solution will be selected. This approach is termed model-driven because the solution selection logic is entirely dependent on the prior error model. Because the EPIC and GERAFS algorithms attempt to bound IR using the *a priori* distribution, they are inherently conservative. Their conservatism arises from the need to protect against

potentially-incorrect fixes without the benefit of conditioning on the observed carrier phase measurements.

In contrast to the model-driven approach, data-driven methods decide *a posteriori* whether to accept the fixed or float solution. Conditioning the selection on the observed measurements reduces the risk of incorrect fixing. A subset of data-driven methods is called integer aperture (IA) estimation [7]. In IA methods, the integer ambiguity vector is estimated, typically using either integer bootstrapping [8] or integer least squares (ILS) [9]. Many IA methods compute a test statistic from the ambiguity residual, i.e., the difference between the float and fixed ambiguities. This test statistic is compared to a threshold to decide between the fixed and float solution.

Perhaps the simplest IA method is IA bootstrapping (IAB), which resolves the integer ambiguities via integer bootstrapping and then tests the fixed solution by applying bootstrapping to a scaled-up version of the ambiguity residual [10]. If the test returns the zero vector, then the fixed solution is selected; otherwise the float solution is selected. IAB is sub-optimal in the sense that bootstrapping does not always find the maximum likelihood integer ambiguity, as opposed to ILS, which is guaranteed to do so. It is also sub-optimal in the sense that it does not maximize the probability of successfully fixing the ambiguities for a given probability of incorrectly fixing them. But it has the advantage that all of these probabilities have analytically computable values, which allows the decision threshold to be set analytically as a function of \bar{P}_F . More generally, IAB enables the strict performance requirements that safety-of-life applications demand to be provably satisfied.

The remaining IA methods discussed in this introduction solve for the integer ambiguity with ILS, which is optimal in the maximum likelihood sense for Gaussian measurement noise. Ellipsoidal IA takes the covariance weighted norm of the ILS ambiguity residual as its test statistic [11]. As with IAB, the simplicity of this statistic allows the decision threshold to be set analytically so long as adjacent apertures do not overlap, but the probability of successfully fixing the ambiguities is sub-optimal. While ellipsoidal IA can have a higher probability of success than IAB for models with a few ambiguities of approximately equal conditional variance, IAB tends to provide a higher probability of success for models in which the conditional variances of the ambiguities differ by more than about 10%, which tends to be the case for realistic measurement models.

Other ILS-based IA methods employ test statistics that are a function of the ambiguity residuals of the ILS fix and of one or more higher-cost alternate fixes. These include the ratio test

[12], [13], the difference test [14], [15], and the optimal test [16], [17]. Unlike IA bootstrapping and ellipsoidal IA, none of these methods' test statistics has an analytical probability distribution or decision threshold [18]. In practice, decision thresholds are set based on one of a few *ad hoc* methods. The crudest of these, which applies a fixed threshold for all measurement models, does not allow one to control the actual probability of incorrect fix, P_F , for time-varying measurement models. More sophisticated methods determine the decision threshold that approximately satisfies \bar{P}_F via Monte Carlo simulation, lookup tables [13], or functional approximations [19], [20]. But these techniques are inapt for safety-of-life systems because the resulting thresholds cannot be analytically proven to satisfy \bar{P}_F for any particular model. At best, they incorporate sufficient conservatism to protect the solution at the expense of decreased availability. Of course, in the limit as the number of test points becomes exceedingly large, Monte Carlo simulation for a given measurement model can yield an arbitrarily exact decision threshold, but such simulation is hardly feasible for real-time operation.

The optimal IA algorithm uses ILS to optimally estimate the ambiguities and then takes as its test statistic the *a posteriori* probability of correct fix [21]. Counterintuitively, the threshold corresponding to a particular \bar{P}_F for this statistic is not analytically computable. Also, the optimal IA estimator involves an infinite sum over all possible integer ambiguities. The search can be truncated once a sufficiently large number of integer fixes has been evaluated, but the number required depends on the strength of the model and on the required \bar{P}_F . To satisfy the most demanding integrity requirements, the search often extends to several hundred candidate fixes in realistic scenarios, which becomes impractical for real-time applications.

This paper's focus on IAB is motivated by the alternative IA approaches' computational complexity or lack of an analytical connection between \bar{P}_F and the decision threshold.

This paper extends the IAB technique to a generalized form in which subsets of the full set of integer ambiguities are considered for resolution if the full set cannot be resolved confidently. This generalization makes IAB a member of the family of Generalized Integer Aperture (GIA) estimators [22]. These algorithms evaluate successively smaller subsets until either a satisfactory fix is found or the float solution is applied as a last resort. Also known as partial ambiguity resolution (PAR), this technique provides gradual degradation of performance for weak models.

In summary, to meet the increasingly stringent performance requirements of safety-of-life applications there is a need for a data-driven ambiguity resolution and validation method whose decision threshold for choosing between a fixed and float solution can be set analytically for a desired \bar{P}_F . To maximize availability, the method must be generalized to accommodate PAR. Extant methods in the high-integrity CDGNSS literature do not satisfy this need.

This paper offers three contributions to address this need. First, IAB is extended to encompass PAR. The extended technique is called Generalized Integer Aperture Bootstrapping (GIAB). Second, analytical characterizations of the probability

of incorrect fix, correct partial fix, and correct full fix are developed and validated. Third, a method for setting the integer aperture size and shape is developed that enables GIAB's availability to exceed IAB's subject to a given \bar{P}_F . These contributions are validated with a set of Monte Carlo simulations, and algorithm performance is compared to the optimal IA, ellipsoidal IA, and IAB methods.

A preliminary version of this work was presented in [23]. This work extends the preliminary work with further validation of the theoretical results via additional simulation of a larger set of measurement models and a detailed comparison to the optimal integer aperture method. A further extension of the preliminary work will be published in a companion paper to this one [24]. The companion paper analytically develops the prior and posterior probability density functions for the GIAB baseline, bounds the integrity risk associated with data-driven PAR, and validates the derived distributions via Monte-Carlo simulation.

The following acronyms will be used frequently throughout the remainder of this paper and are collected here for ease of reference: IA - Integer Aperture, IB - Integer Bootstrapping, IAB - Integer Aperture Bootstrapping, and GIAB - Generalized Integer Aperture Bootstrapping.

II. GENERALIZED INTEGER APERTURE BOOTSTRAPPING

A. Integer Bootstrapping Overview

The basic theory of integer bootstrapping (IB) is reproduced here from [8] with a few amplifications for ease of understanding and notational consistency. The treatment begins with the linearized, short-baseline GNSS measurement model

$$\mathbf{y} = B\mathbf{b} + A\mathbf{a} + \boldsymbol{\nu} \quad (1)$$

where $\mathbf{y} \in \mathbb{R}^n$ contains the "observed-minus-modeled" double-difference carrier-phase and, optionally, pseudorange measurements, $\mathbf{b} \in \mathbb{R}^3$ is the unknown, real-valued correction to the modeled baseline between GNSS antennas, $\mathbf{a} \in \mathbb{Z}^m$ holds the unknown carrier phase integer ambiguities, B and A are appropriately-dimensioned measurement sensitivity matrices, and $\boldsymbol{\nu} \in \mathbb{R}^n$ is the zero-mean, double-difference measurement noise with variance $Q_{\mathbf{y}}$.

Applying weighted least squares estimation to (1), with $H = [B \ A]$, produces real-valued estimates of \mathbf{b} and \mathbf{a} :

$$\begin{bmatrix} \hat{\mathbf{b}} \\ \hat{\mathbf{a}} \end{bmatrix} = (H^T Q_{\mathbf{y}}^{-1} H)^{-1} H^T Q_{\mathbf{y}}^{-1} \mathbf{y} \quad (2a)$$

$$E \left(\begin{bmatrix} \hat{\mathbf{b}} \\ \hat{\mathbf{a}} \end{bmatrix} \right) = \begin{bmatrix} \mathbf{b} \\ \mathbf{a} \end{bmatrix} \quad (2b)$$

$$\text{cov} \left(\begin{bmatrix} \hat{\mathbf{b}} \\ \hat{\mathbf{a}} \end{bmatrix} \right) = \begin{bmatrix} Q_{\hat{\mathbf{b}}} & Q_{\hat{\mathbf{b}}\hat{\mathbf{a}}} \\ Q_{\hat{\mathbf{a}}\hat{\mathbf{b}}} & Q_{\hat{\mathbf{a}}} \end{bmatrix} = (H^T Q_{\mathbf{y}}^{-1} H)^{-1} \quad (2c)$$

The estimates $\hat{\mathbf{a}} \in \mathbb{R}^m$ and $\hat{\mathbf{b}} \in \mathbb{R}^3$, called the float ambiguity and float baseline, ignore the integer constraint $\mathbf{a} \in \mathbb{Z}^m$.

Integer ambiguity resolution is a technique by which the float ambiguity $\hat{\mathbf{a}}$ is mapped to a vector of integers $\tilde{\mathbf{a}} \in \mathbb{Z}^m$. The process can be represented by the map

$$\tilde{\mathbf{a}} = M(\hat{\mathbf{a}}, Q_{\hat{\mathbf{a}}}) \quad (3)$$

$$M : \mathbb{R}^m \times \mathbf{S}_{++}^m \mapsto \mathbb{Z}^m$$

where \mathbf{S}_{++}^m is the set of positive definite matrices of size $m \times m$. The integer-bootstrapping variant of M operates in such a way that when $Q_{\hat{\mathbf{a}}}$ has non-zero off-diagonal elements, the probability that $\hat{\mathbf{a}} = \mathbf{a}$ depends on the ordering of the elements of $\hat{\mathbf{a}}$ [8]. To ensure near-optimal IB performance, an integer-preserving transformation is applied to decorrelate, insofar as possible, the elements of $\hat{\mathbf{a}}$; details of this transformation, referred to as the Z-transform, may be found in [25], [26]. The decorrelated float ambiguity is $\hat{\mathbf{z}} = Z^T \hat{\mathbf{a}}$, and the transformed true ambiguity is $\mathbf{z} = Z^T \mathbf{a}$, with Z being the integer-preserving transformation matrix. Likewise, $Q_{\hat{\mathbf{a}}}$ and $Q_{\hat{\mathbf{b}}\hat{\mathbf{a}}}$ are transformed as $Q_{\hat{\mathbf{z}}} = Z^T Q_{\hat{\mathbf{a}}} Z$ and $Q_{\hat{\mathbf{b}}\hat{\mathbf{z}}} = Q_{\hat{\mathbf{b}}\hat{\mathbf{a}}} Z$. All integer-related operations hereafter will be performed in the decorrelated space, with $\hat{\mathbf{z}}$ referred to as the float ambiguity.

The functional map $M(\hat{\mathbf{z}}, Q_{\hat{\mathbf{z}}})$ partitions \mathbb{R}^m into disjoint subsets, called pull-in regions, that collectively cover \mathbb{R}^m . Each region is an integer-valued translation of the subset

$$S_0 \triangleq \{\mathbf{x} \in \mathbb{R}^m \mid \mathbf{0} = M(\mathbf{x}, Q_{\mathbf{x}})\} \quad (4)$$

The pull-in region $S_{\zeta} \subset \mathbb{R}^m$ is the set of all points \mathbf{x} mapped by $M(\mathbf{x}, Q_{\mathbf{x}})$ to the integer vector $\zeta \in \mathbb{Z}^m$:

$$\begin{aligned} S_{\zeta} &\triangleq \{\mathbf{x} \in \mathbb{R}^m \mid \zeta = M(\mathbf{x}, Q_{\mathbf{x}})\}, \quad \zeta \in \mathbb{Z}^m \\ S_{\zeta} &= S_0 + \zeta \end{aligned} \quad (5)$$

For IB, the pull-in regions are m -dimensional parallelotopes centered on the integers.

For presentation of the IB algorithm, it will be convenient to decompose the covariance of the float ambiguity as $Q_{\hat{\mathbf{z}}} = LDL^T$, where L is a unit lower triangular matrix and D is a diagonal matrix, and to model the float ambiguity as the true ambiguity plus zero-mean Gaussian noise, $\hat{\mathbf{z}} = \mathbf{z} + \epsilon$, $\epsilon \sim \mathcal{N}(0, Q_{\hat{\mathbf{z}}})$. Multiplication by L^{-1} transforms ϵ into a vector whose elements are mutually uncorrelated: $\epsilon_{\mathbf{c}} \triangleq L^{-1}\epsilon$, $\epsilon_{\mathbf{c}} \sim \mathcal{N}(0, D)$. Letting l_{ij} denote the ij th element of L , d_i the i th element of the diagonal of D , and ϵ_i and ϵ_{ci} the i th elements of ϵ and $\epsilon_{\mathbf{c}}$, respectively, ϵ_i and its variance can be computed from the first i components of $\epsilon_{\mathbf{c}}$ as

$$\epsilon_i = \sum_{k=1}^i l_{ik} \epsilon_{ck}, \quad \text{var}(\epsilon_i) = \sum_{k=1}^i l_{ik}^2 d_k \quad (6)$$

IB can be interpreted as constrained maximum likelihood estimation in which the integer constraint $\mathbf{z} \in \mathbb{Z}^m$ is applied sequentially. Application of the integer constraint can also be viewed as conditioning on an assumed value of ϵ . For convenience in what follows, let the shorthand notation \mathbf{v}_I denote the vector composed of the first $i-1$ elements of any vector \mathbf{v} of sufficient length. Thus, $\epsilon_I = [\epsilon_1, \dots, \epsilon_{i-1}]^T$. Let $\epsilon_j | \epsilon_I$ represent the j th element of ϵ conditioned on ϵ_I being known. Starting with (6), and exploiting the lack of correlation in the elements of $\epsilon_{\mathbf{c}}$, one can show that

$$\epsilon_j | \epsilon_I \sim \mathcal{N} \left(\sum_{k=1}^{i-1} l_{jk} \epsilon_{ck}, \sum_{k=i}^j l_{jk}^2 d_k \right), \quad j = i, \dots, m \quad (7)$$

Note that $\text{var}(\epsilon_i | \epsilon_I) = d_i$. Thus, d_i can be interpreted as the conditional variance of the i th ambiguity. A larger value of d_i indicates that correct integer resolution of the i th ambiguity will be more difficult.

One may alternatively find the mean of $\epsilon_j | \epsilon_I$ via the standard expression for conditional mean. Assume $\epsilon_I \sim \mathcal{N}(0, Q_I)$, and let $Q_{jI} \in \mathbb{R}^{1 \times (i-1)}$ be the cross-correlation matrix between ϵ_j and ϵ_I , for $j \geq i$. Then the mean of ϵ_j conditioned on knowledge of ϵ_I is [27]

$$E[\epsilon_j | \epsilon_I] = Q_{jI} Q_I^{-1} \epsilon_I \quad (8)$$

With these preliminaries, the algorithm for a single step of IB is straightforward. Let $\mathbf{z}_I = [z_1, \dots, z_{i-1}]^T$, and suppose that one assumes $\mathbf{z}_I = \check{\mathbf{z}}_I$ for some known $\check{\mathbf{z}}_I = [\check{z}_1, \dots, \check{z}_{i-1}]^T \in \mathbb{Z}^{i-1}$. Then, starting from $\hat{\mathbf{z}} = \mathbf{z} + \epsilon$, the constrained maximum likelihood estimate of z_i given $\mathbf{z}_I = \check{\mathbf{z}}_I$ is

$$\hat{z}_{i|I} = \hat{z}_i - Q_{iI} Q_I^{-1} (\hat{\mathbf{z}}_I - \check{\mathbf{z}}_I) \quad (9)$$

Defining $\check{\epsilon} \triangleq \hat{\mathbf{z}} - \check{\mathbf{z}}$ and $\check{\epsilon}_{\mathbf{c}} \triangleq L^{-1} \check{\epsilon}$, and referencing (7) and (8), one recognizes (9) as equivalent to

$$\begin{aligned} \hat{z}_{i|I} &= \hat{z}_i - E[\epsilon_i | \epsilon_I = \check{\epsilon}_I] \\ &= \hat{z}_i - \sum_{k=1}^{i-1} l_{ik} \check{\epsilon}_{ck} \\ &= z_i + \sum_{k=1}^i l_{ik} \epsilon_{ck} - \sum_{k=1}^{i-1} l_{ik} \check{\epsilon}_{ck} \end{aligned} \quad (10)$$

where the last equality makes use of $\hat{z}_i = z_i + \epsilon_i$ and (6). The quantities $\hat{z}_{i|I}$, $i = 1, 2, \dots, m$ are called the sequentially-constrained float ambiguity estimates; these are stacked to form the vector $\hat{\mathbf{z}}_{\mathbf{c}}$.

It is shown in Appendix A that $\check{\epsilon}_{\mathbf{c}} = \hat{\mathbf{z}}_{\mathbf{c}} - \check{\mathbf{z}}$, which evokes an interpretation of $\check{\epsilon}_{\mathbf{c}}$ as the sequentially-constrained ambiguity residual. When $\check{\epsilon}_{ci}$, the i th element of $\check{\epsilon}_{\mathbf{c}}$, is small, this implies that the sequentially-constrained float estimate $\hat{z}_{ci} = \hat{z}_{i|I}$ is close to \check{z}_i , meaning the assumption $z_i = \check{z}_i$ is likely correct. If the assumption is correct for all z_k , $k \in \{1, \dots, i-1\}$, then $\epsilon_{ck} = \check{\epsilon}_{ck}$ for all $k \in \{1, \dots, i-1\}$, and (10) simplifies to

$$\hat{z}_{i|I} = z_i + \epsilon_{ci} \quad (11)$$

The appearance of ϵ_{ci} as the sole noise element in this equation indicates that, given the true value of \mathbf{z}_I , $\hat{z}_{i|I}$ is uncorrelated with ϵ_I , and, by extension, with $\hat{\mathbf{z}}_I$. This important property allows the integer constraint $z_i \in \mathbb{Z}$ to be enforced directly on $\hat{z}_{i|I}$ by simple rounding, yielding the conditional maximum-likelihood integer estimate

$$\check{z}_i = \lfloor \hat{z}_{i|I} \rfloor \quad (12)$$

where $\lfloor \cdot \rfloor$ denotes nearest integer rounding. The set of successively-obtained integer estimates are stacked to form the vector $\check{\mathbf{z}} = [\check{z}_1, \dots, \check{z}_m]^T$, which is called the fixed ambiguity, as distinguished from the float ambiguity $\hat{\mathbf{z}}$. Note that, if one or more of the elements in \mathbf{z}_I are constrained incorrectly, so that the integer error vector $\Delta \mathbf{z}_I \triangleq \check{\mathbf{z}}_I - \mathbf{z}_I$ is nonzero, then (10) instead becomes

$$\hat{z}_{i|I} = z_i + \epsilon_{ci} + \sum_{k=1}^{i-1} l_{ik} \Delta z_k \quad (13)$$

where Δz_k is the k th element of $\Delta \mathbf{z}_I$.

To summarize, the i th IB iteration starts by assuming $\mathbf{z}_I = \hat{\mathbf{z}}_I$, calculates $\hat{z}_{i|I}$ subject to this constraint as in the center equation in (10), then rounds $\hat{z}_{i|I}$ to the nearest integer to obtain \tilde{z}_i . The full IB algorithm becomes clear by mention of two additional points: (1) $\hat{\mathbf{z}}_I$ is taken to be composed of the integer-rounded estimates from previous steps, and (2) for $i = 1$, $\hat{z}_{i|I} = \hat{z}_i$.

An efficient implementation of IB is given in pseudocode below. This implementation, which is functionally equivalent to that given in [8] although its internal details differ, is the starting point for the new algorithm developed in this paper.

Algorithm 1: IB($\hat{\mathbf{z}}, L$)

Input : $\hat{\mathbf{z}} \in \mathbb{R}^m$, $L \in \mathbb{R}^{m \times m}$

Output: $\tilde{\mathbf{z}} \in \mathbb{Z}^m$

```

1  $\hat{\mathbf{z}}_c = \hat{\mathbf{z}}$ 
2 for  $i = 1:m$  do
3    $\tilde{z}_i = \lfloor \hat{z}_{ci} \rfloor$ 
4    $\check{\epsilon}_{ci} = \hat{z}_{ci} - \tilde{z}_i$ 
5   for  $j = i+1:m$  do
6      $\hat{z}_{cj} = \hat{z}_{cj} - l_{ij}\check{\epsilon}_{ci}$ 
7   end
8 end

```

Once the fixed ambiguity $\tilde{\mathbf{z}}$ is computed, an integer-constrained baseline estimate, called the fixed baseline, is produced as

$$\begin{aligned} \check{\mathbf{b}} &= \hat{\mathbf{b}} - Q_{\hat{\mathbf{b}}\tilde{\mathbf{z}}} Q_{\tilde{\mathbf{z}}}^{-1} \check{\epsilon} \\ &= \hat{\mathbf{b}} - Q_{\hat{\mathbf{b}}\tilde{\mathbf{z}}} L^{-T} D^{-1} \check{\epsilon}_c \end{aligned} \quad (14)$$

The corresponding covariance matrix reflects the improved precision of the baseline estimate due to integer fixing, assuming all ambiguities were fixed correctly:

$$Q_{\check{\mathbf{b}}} = Q_{\hat{\mathbf{b}}} - Q_{\hat{\mathbf{b}}\tilde{\mathbf{z}}} Q_{\tilde{\mathbf{z}}}^{-1} Q_{\tilde{\mathbf{z}}\hat{\mathbf{b}}}^T \quad (15)$$

B. Integer Aperture Bootstrapping (IAB)

IAB extends the IB concept by adding a validation test [10]. The test statistic for IAB can be expressed as a function of the ambiguity residual $\check{\epsilon} \triangleq \hat{\mathbf{z}} - \tilde{\mathbf{z}}$ and a parameter $\beta \in [0, 1]$ called the aperture parameter:

$$T(\check{\epsilon}, L, \beta) = \left\| \text{IB} \left(\frac{1}{\beta} \check{\epsilon}, L \right) \right\|_0 \quad (16)$$

Here, $\|\mathbf{v}\|_0 \triangleq |\{i \mid v_i \neq 0\}|$ denotes the number of non-zero elements in the vector \mathbf{v} . It can be shown that $T(\check{\epsilon}, L, \beta) = 0 \iff |\check{\epsilon}_{ci}| < \frac{\beta}{2}, \forall i \in \{1, \dots, m\}$ [10]. Thus, a small β ensures that $T(\check{\epsilon}, L, \beta) = 0$ only when the sequentially-constrained ambiguity residuals are small, implying that $\tilde{\mathbf{z}} = \mathbf{z}$ with high probability. Accordingly, IAB accepts the integer fix produced by IB whenever $T = 0$, but otherwise rejects it. In the event that the fix is rejected, IAB resorts to the float solution $\hat{\mathbf{z}}$. The overall IAB process can be represented by the map

$$\text{IAB}(\hat{\mathbf{z}}, L, \beta) \triangleq \begin{cases} \text{IB}(\hat{\mathbf{z}}, L) & \text{if } T(\check{\epsilon}, L, \beta) = 0 \\ \hat{\mathbf{z}} & \text{otherwise} \end{cases}$$

Note that, since $\text{IB}(\check{\epsilon}, L) = \mathbf{0}$, a fixed solution can be forced by choosing $\beta = 1$; likewise, a float solution is forced by $\beta = 0$.

The set of all float ambiguities mapped to the vector ζ , called Ω_ζ , is a subset of the corresponding pull-in region of $\text{IB}(\hat{\mathbf{z}}, L)$, with equality if and only if $\beta = 1$:

$$\begin{aligned} \Omega_\zeta &= \{\mathbf{x} \in \mathbb{R}^m \mid \zeta = \text{IAB}(\mathbf{x}, L, \beta)\}, \zeta \in \mathbb{Z}^m \\ \Omega_\zeta &\subseteq S_\zeta \end{aligned} \quad (17)$$

Such sets are called apertures. Due to the integer invariance of integer bootstrapping, $\Omega_\zeta = \Omega_0 + \zeta$.

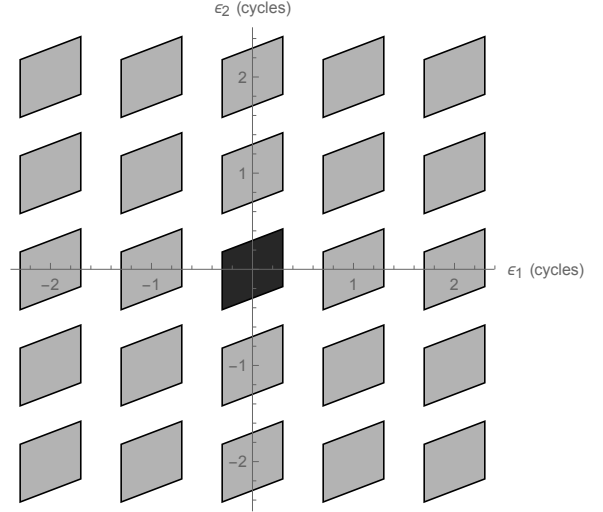


Fig. 1. IAB aperture regions for a two-dimensional example model. This is a visual representation of the possible outcomes of $\text{IAB}(\epsilon, L, \beta)$. The axes correspond to the first to float ambiguity errors in units of cycles. The central, darkly shaded region is the success region, in which $\tilde{\mathbf{z}} = \mathbf{z}$. The lightly shaded regions correspond to incorrect ambiguity fixes, in which $\tilde{\mathbf{z}} \neq \mathbf{z}$. The unshaded region is the fix-rejection region.

The IAB apertures have the same shape as the IB pull-in region but are scaled by a factor of β . Accordingly, gaps between integer-shifted apertures emerge whenever $\beta < 1$, as illustrated in Fig. 1. Three important regions can be identified in Fig. 1, each corresponding to a possible IAB outcome. The central, dark region corresponds to the success event in which the full ambiguity set is resolved correctly. The union of the many lightly shaded regions corresponds to the failure event in which one or more integer ambiguities are fixed incorrectly. Values of $\epsilon = \hat{\mathbf{z}} - \mathbf{z}$ falling in the unshaded region result in the fix being rejected. This is the undecided event. The probabilities of these events are [10], [28]

$$P_S = \prod_{i=1}^m \left(2\Phi \left(\frac{\beta/2}{\sqrt{d_i}} \right) - 1 \right) \quad (18a)$$

$$P_F = \sum_{\tilde{\mathbf{z}} \in \mathbb{Z}^m \setminus \{0\}} \prod_{i=1}^m \left(\Phi \left(\frac{\beta/2 - L^i \tilde{\mathbf{z}}}{\sqrt{d_i}} \right) - \Phi \left(\frac{-\beta/2 - L^i \tilde{\mathbf{z}}}{\sqrt{d_i}} \right) \right) \quad (18b)$$

$$P_U = 1 - P_F - P_S \quad (18c)$$

where L^i is the i th row of L^{-1} , and $\Phi(\cdot)$ is the CDF of the standard normal random variable.

A few observations should be made about the event probabilities. First, calculation of P_F involves an infinite sum over all integer ambiguities other than the correct one. One can calculate an approximate P_F by summing over a large number of alternative ambiguities, but this may still be computationally expensive if the specified acceptable P_F , written \bar{P}_F , is small or if m is large. Second, P_F is a monotonically increasing function of β , which implies that P_F decreases as the integer aperture is made smaller. Thus, the aperture parameter β controls the failure probability. Third, P_S is also monotonically increasing in β , which implies that any increase in P_S comes at the expense of an increase in P_F .

C. Generalization to Partial Ambiguity Resolution

Accepting or rejecting the whole of \check{z} , as IAB does, is an extreme approach that limits the range of useful outcomes. Consider instead a variant of IAB in which a subset of the elements of \check{z} may be accepted. IAB is well suited to such generalization from full to partial ambiguity resolution, for two reasons. First, the lack of correlation between the elements of $\check{\epsilon}_c$ allows an aperture test to be applied separately to each element. Moreover, the test can be tailored for each element: the i th ambiguity can be tested against aperture parameter β_i , with the vector $\beta = [\beta_1, \dots, \beta_m]^T$ chosen such that $P_F \leq \bar{P}_F$. A later section will discuss the benefits of such element-specific aperture sizing.

Second, one need not consider every possible subset of IAB ambiguities, which, besides being computationally demanding, would involve so many aperture tests that the probability of one of them randomly passing will force the selection of small β_i values to satisfy $P_F \leq \bar{P}_F$. These small β_i will lead to the rejection of many correct fixes, driving down P_S . Instead, one can achieve good performance even when considering only the subset corresponding to the first $q \leq m$ elements of \hat{z} , where q is the number that pass the validation test. This is because any of the commonly-accepted Z transform techniques (e.g., those in [25], [26]) tend to arrange \hat{z} to greatly increase (though not necessarily maximize) P_S relative to what would have been possible with the un-transformed system. And since the expected value of q can be shown to increase with P_S , attempted fixing from the first to last element of \hat{z} ensures that q will be maximized, or nearly so.

The new algorithm, called generalized integer aperture bootstrapping (GIAB), is given in pseudocode below. GIAB successively fixes ambiguities until it determines that the next one cannot be fixed without P_F exceeding \bar{P}_F . The output q is the number of ambiguities fixed; $q < m$ implies the $(q+1)$ th validation test failed, so the last $m - q$ ambiguities were left unfixed.

Whereas IAB has three outcome events (success, failure, and undecided), GIAB has $m+2$. These are defined in terms of the random variables \check{z} and q as follows, where $\mathbf{z}_{1:n}$ indicates the vector composed of the first n elements of the vector \mathbf{z} :

$$F : \check{z}_{1:q} \neq \mathbf{z}_{1:q}, \quad q \in \{1, \dots, m\} \quad (19a)$$

$$U : q = 0 \quad (19b)$$

$$S_i : \check{z}_{1:i} = \mathbf{z}_{1:i}, \quad q = i \in \{1, \dots, m\} \quad (19c)$$

Algorithm 2: GIAB (\hat{z}, L, β)

Input : $\hat{z} \in \mathbb{R}^m, L \in \mathbb{R}^{m \times m}, \beta \in [0, 1]^m$
Output: $q \in \{0, \dots, m\}, \check{z} \in \mathbb{Z}^{\min(q+1, m)}$

```

1  $q = 0$ 
2  $\check{z}_c = \hat{z}$ 
3 for  $i = 1:m$  do
4    $\check{z}_i = \lfloor \hat{z}_{ci} \rfloor$ 
5    $\check{\epsilon}_{ci} = \hat{z}_{ci} - \check{z}_i$ 
6   if  $|\check{\epsilon}_{ci}| < \frac{\beta_i}{2}$  then
7      $q = i$ 
8     for  $j = i+1:m$  do
9        $\check{z}_{cj} = \hat{z}_{cj} - l_{ji}\check{\epsilon}_{ci}$ 
10    end
11  else
12    break
13  end
14 end

```

The failure event F occurs upon acceptance of any incorrect integers. The undecided event U occurs when no ambiguity is fixed. There are m success events S_i defined for each possible number of correct integer fixes from 1 to m .

The aperture $\Omega_\zeta \subset \mathbb{R}^m, \zeta \in \mathbb{Z}^m$, introduced in (17) for IAB, can be generalized for partial ambiguity resolution as $\Omega_{i,\zeta} \subset \mathbb{R}^m, \zeta \in \mathbb{Z}^i, i \in \{1, \dots, m\}$. Let \check{x} and q be the outputs of GIAB (\mathbf{x}, L, β). Then

$$\Omega_{i,\zeta} = \{\mathbf{x} \in \mathbb{R}^m \mid \zeta = \check{\mathbf{x}}_{1:i}, q = i\}, \quad i \in \{1, \dots, m\}, \zeta \in \mathbb{Z}^i \quad (20)$$

In other words, $\Omega_{i,\zeta}$ is the set of all float ambiguity vectors whose first i elements are mapped and validated by GIAB to $\zeta \in \mathbb{Z}^i$, but whose $(i+1)$ th element is not validated. Note that when $\beta_i = \beta$ for all $i \in \{1, \dots, m\}$, then $\Omega_{m,\zeta} = \Omega_\zeta, \zeta \in \mathbb{Z}^m$.

The success event S_i can be defined in terms of $\Omega_{i,\zeta}$ as

$$S_i : \hat{z} \in \Omega_{i,\zeta}, \quad i \in \{1, \dots, m\} \quad (21)$$

and the failure event can be defined as

$$F : \hat{z} \in \left\{ \bigcup_{i \in \{1, \dots, m\}} \left(\bigcup_{\zeta \in \mathbb{Z}^i \setminus \mathbf{z}_{1:i}} \Omega_{i,\zeta} \right) \right\} \quad (22)$$

The regions corresponding to the F, U , and S_i events are illustrated in Fig. 2 for $m = 2$.

D. Partial Ambiguity Resolution Probabilities

To assess GIAB's theoretical performance, the probability of each possible event must be computed. For the i th ambiguity reached during GIAB processing, there are three possibilities: the fix is accepted correctly, accepted erroneously, or rejected. Conditioned on the event that the first $i - 1$ integers have been

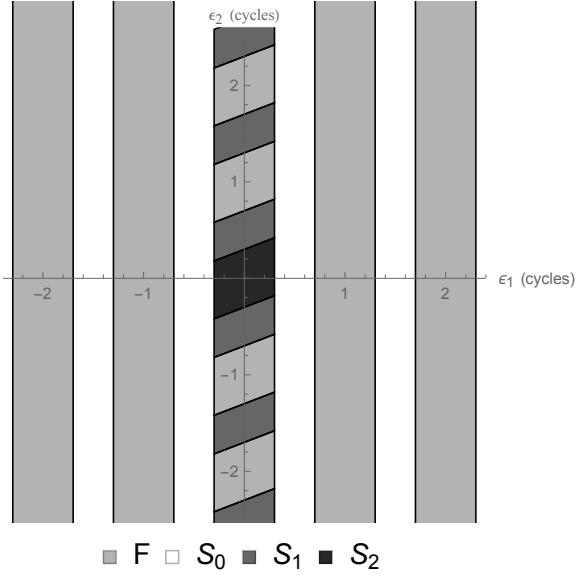


Fig. 2. Regions of the float ambiguity error, $\epsilon \in \mathbb{R}^m$, that are mapped by GIAB to failure, undecided, and success events for an example model with $m = 2$. The axes correspond to the first to float ambiguity errors in units of cycles. Event F results if one or more ambiguities are fixed incorrectly. Event S_i occurs when exactly $i \in \{1, \dots, m\}$ ambiguities are fixed and each of these is correct. Event U occurs when the first ambiguity is rejected, leaving all ambiguities unfixed.

fixed correctly (i.e., $\check{z}_I = z_I$), the probabilities for these three events, for $i \in \{1, \dots, m\}$, follow from (18):

$$P_{C_i} = P\left(|\epsilon_{ci}| < \frac{\beta_i}{2} \mid \check{z}_I = z_I\right) = 2\Phi\left(\frac{\beta_i/2}{\sqrt{d_i}}\right) - 1 \quad (23a)$$

$$\begin{aligned} P_{E_i} &= \sum_{\zeta \in \mathbb{Z} \setminus \{0\}} P\left(|\epsilon_{ci} - \zeta| < \frac{\beta_i}{2} \mid \check{z}_I = z_I\right) \\ &= \sum_{\zeta \in \mathbb{Z} \setminus \{0\}} \left(\Phi\left(\frac{\beta_i/2 - \zeta}{\sqrt{d_i}}\right) - \Phi\left(\frac{-\beta_i/2 - \zeta}{\sqrt{d_i}}\right) \right) \end{aligned} \quad (23b)$$

$$P_{R_i} = P\left(\frac{\beta_i}{2} \leq |\epsilon_{ci}| \mid \check{z}_I = z_I\right) = 1 - P_{E_i} - P_{C_i} \quad (23c)$$

Note that, for $i = 1$, \check{z}_I and z_I become empty vectors and the conditioning has no effect.

The failure event probability, P_F , is computed by noting that one or more fixing errors entail the failure event and that, if an ambiguity is rejected, no further ambiguities are considered. Thus P_{E_i} only contributes to P_F if all previous ambiguities were fixed correctly. The probability of the i th success event, P_{S_i} , can be computed by applying similar logic. The probability of the undecided event, P_U , is simply P_{R1} .

The failure, success, and undecided probabilities are thus

$$P_F = P_{E1} + \sum_{i=2}^m P_{E_i} \prod_{j=1}^{i-1} P_{C_j} \quad (24a)$$

$$P_{S_i} = \begin{cases} \prod_{j=1}^m P_{C_j} & i = m \\ P_{R(i+1)} \prod_{j=1}^i P_{C_j} & i \in \{1, \dots, m-1\} \end{cases} \quad (24b)$$

$$P_U = P_{R1} \quad (24c)$$

Note that if $\beta_i = \beta$ for all $i \in \{1, \dots, m\}$, then P_{S_m} is equal to P_S as defined for IAB in (18a).

A bound can be introduced to avoid the infinite sum in calculating P_{E_i} . Consider the region $\frac{\beta_i}{2} \leq |\epsilon_{ci}| \leq 1 - \frac{\beta_i}{2}$, which is a subset of the rejection region $\frac{\beta_i}{2} \leq |\epsilon_{ci}|$, so that $P_{R_i} \geq P\left(\frac{\beta_i}{2} \leq |\epsilon_{ci}| \leq 1 - \frac{\beta_i}{2} \mid \check{z}_I = z_I\right)$. Appending to this region the correct acceptance region $|\epsilon_{ci}| < \frac{\beta_i}{2}$ from (23a), and working out the probability for the combined region, it follows that

$$P_{C_i} + P_{R_i} \geq 1 - 2\Phi\left(\frac{\beta_i/2 - 1}{\sqrt{d_i}}\right) \quad (25)$$

From this and (23c), one obtains the following upper bound on P_{E_i} :

$$P_{E_i} \leq 2\Phi\left(\frac{\beta_i/2 - 1}{\sqrt{d_i}}\right) \quad (26)$$

Provided \bar{P}_F is small and the measurement model is strong enough that $\sqrt{d_i} < 0.2$, as is typical, this bound on P_{E_i} is tight. The next section invokes the bound, together with \bar{P}_F , to set the aperture parameters β_i .

III. SETTING THE INTEGER APERTURE PARAMETERS

In IAB, P_F is controlled by adjusting a single aperture parameter β . GIAB is more flexible, as it allows a tailored parameter β_i for each validation test. For any specified \bar{P}_F , a parameter vector $\beta = [\beta_1, \dots, \beta_m]^T$ can almost always be found so that GIAB's probability of fixing all m integers, P_{S_m} , exceeds IAB's P_S . This section shows how β can be computed analytically to satisfy $P_F \leq \bar{P}_F$, and develops a technique that chooses β to nearly maximize P_{S_m} .

A. Allocation from Probability of Failure

Each validation test that GIAB performs contributes to P_F . The parameter β_i determines the amount of incorrect fixing risk that gets allocated to i th ambiguity, from an overall risk budget \bar{P}_F . (The word *risk* here and elsewhere in this paper refers to the probability of an undesirable event.) Suppose $w_i \bar{P}_F$ is allocated to the i th ambiguity, where $w_i < 1$, and suppose the aperture parameters preceding β_i have all been set, which implies that P_{C_j} is known for all $j \in \{1, \dots, i-1\}$. Then the maximum allowable β_i —the one that maximizes P_{S_i} subject to the allocation $w_i \bar{P}_F$ —is found in two steps. First, P_{E_i} is written as a function of $w_i \bar{P}_F$ by isolating its contribution to P_F in (24a):

$$P_{E_i}(w_i \bar{P}_F) = \begin{cases} w_1 \bar{P}_F & i = 1 \\ \frac{w_i \bar{P}_F}{\prod_{j=1}^{i-1} P_{C_j}} & i = 2, \dots, m \end{cases} \quad (27)$$

Second, the corresponding value of β_i is found by treating (26) as an equality and inverting it to find β_i . Applying the constraint $\beta_i \in [0, 1]$, one has $\beta_i = \beta_{\max}(P_{Ei}, d_i)$, with

$$\beta_{\max}(P_{Ei}, d_i) \triangleq \min \left[1, \max \left[0, 2 \left(1 + \sqrt{d_i} \Phi^{-1}(P_{Ei}/2) \right) \right] \right]$$

Note that if any $\beta_i = 0$, then the i th and following ambiguities cannot be fixed while satisfying $P_F \leq \bar{P}_F$. Conversely, if $\beta_i = 1$ for all $i \in \{1, \dots, m\}$, then all m ambiguities can be fixed while satisfying $P_F \leq \bar{P}_F$.

The functions $P_{Ei}(w_i \bar{P}_F)$ and $\beta_{\max}(P_{Ei}, d_i)$, which are constructed from well-known and readily-computable operations, constitute an analytical mapping from $w_i \bar{P}_F$ to β_i . This analytical relationship is a key benefit of GIAB, as it allows data-driven partial ambiguity resolution to be applied in safety-of-life systems that must provably satisfy $P_F \leq \bar{P}_F$.

B. Optimization for Availability of Full Ambiguity Resolution

Consider how the w_i should be chosen. Assuming a nonzero risk is allocated to each ambiguity, and assuming the full risk budget \bar{P}_F is to be exhausted, the w_i should satisfy

$$0 < w_i < 1, \forall i \in \{1, \dots, m\} \quad \text{and} \quad \sum_{i=1}^m w_i = 1 \quad (28)$$

One could allocate an equal fraction of \bar{P}_F to each of the m ambiguities by setting $w_i = 1/m$ for all $i \in \{1, \dots, m\}$, but this may not be optimal in the sense of maximizing the probability P_{S_m} of correctly resolving all m ambiguities. The optimal allocation problem can be posed in terms of β as

$$\beta^* = \arg \max_{\beta} [P_{S_m}(\beta)] \quad (29)$$

$$\text{s.t. } P_F(\beta) \leq \bar{P}_F \text{ and conditions in (28)}$$

This problem can be approached by gradient ascent, but P_{S_m} and P_F are both non-convex functions of β and give rise to many local maxima in the region of the global maximum. Thus, gradient ascent offers no guarantee of finding the global optimum, besides which the gradient calculation for this problem is computationally expensive.

Mercifully, a nearly-optimal choice of the w_i can be found by a simple heuristic. Because both P_{S_m} and P_F are functions of the conditional variances d_i , it is reasonable to compute the weights as functions of d_i as well. The most general function satisfying (28) is

$$w_i = \frac{f(d_i)}{\sum_{j=1}^m f(d_j)} \quad (30)$$

where $f(d_i)$ is a weighting function. Guided by the intuition that more risk must be allocated to the ambiguities that are most difficult to resolve (those having the largest d_i), lest their resulting small β_i reject fixing too often, four variants of $f(d_i)$, shown in the following table, are considered: Equal-weighting, σ -weighting, σ^2 -weighting, and P_E -weighting. Note that P_E -weighting simply sets $f(d_i)$ equal to P_{Ei} from (26) with $\beta_i = 1$. This heuristic does not ensure the global optimum is found, but offers good performance.

When tested on a variety of models with bootstrap probability of correct fix ranging from .85 to .9999 and for a

TABLE I
WEIGHTING FUNCTION ALTERNATIVES CONSIDERED

	Equal	σ	σ^2	P_E
$f(d_i)$	1	$\sqrt{d_i}$	d_i	$2\Phi\left(\frac{-1/2}{\sqrt{d_i}}\right)$

wide range of \bar{P}_F , it was found that P_E -weighting produces the highest P_{S_m} for all models studied, including cases of flat spectra (e.g., $\max\{d_i\}_1^m / \min\{d_i\}_1^m < 1.1$), and spectra with significant variation (e.g., $\max\{d_i\}_1^m / \min\{d_i\}_1^m > 7$). When performing gradient ascent optimization starting from the P_E -weighted β , or starting from a large number of random initial β distributed across its whole range, there was never observed more than a 0.03% increase in P_{S_m} . Moreover, compared to the common-parameter case in which $\beta_i = \beta$ for all $i \in \{1, \dots, m\}$, the probability P_{S_m} for P_E -weighting was never lower, and almost always higher—often by several percent. P_E -weighting can thus be considered nearly optimal, and is the recommended strategy for aperture sizing. The overall aperture sizing algorithm is given in the following pseudocode. Note that even when the algorithm's output β does not quite maximize P_{S_m} , it nevertheless guarantees $P_F \leq \bar{P}_F$, which is most important for safety-of-life systems.

Algorithm 3: SetBeta (\bar{P}_F, \mathbf{d})

Input : $\bar{P}_F \in [0, 1]$, $\mathbf{d} \in \mathbb{R}^m$
Output: $\beta \in [0, 1]^m$

- 1 $\Sigma = 0$;
- 2 $A = 1$;
- 3 **for** $i = 1:m$ **do**
- 4 $P_{Ei} = 2\Phi\left(-\frac{1/2}{\sqrt{d_i}}\right)$
- 5 $\Sigma = \Sigma + P_{Ei}$
- 6 **end**
- 7 **for** $i = 1:m$ **do**
- 8 $w_i = \frac{P_{Ei}}{\Sigma}$
- 9 $\beta_i = \min\left(\max\left[2\left(1 + \sqrt{d_i}\Phi^{-1}\left(\frac{w_i \bar{P}_F}{2A}\right)\right), 0\right], 1\right)$
- 10 $A = \left(2\Phi\left(\frac{\beta_i/2}{\sqrt{d_i}}\right) - 1\right) A$
- 11 **end**

IV. THE GENERALIZED INTEGER APERTURE BASELINE

Analogous to the float baseline $\hat{\mathbf{b}}$ and the fixed baseline $\check{\mathbf{b}}$, a partially-fixed baseline can be calculated from the inputs and outputs of GIAB. Let (14) be rewritten as

$$\check{\mathbf{b}} = \hat{\mathbf{b}} - \sum_{j=1}^m Q_{\hat{\mathbf{b}} \hat{\mathbf{z}}_c}^j \frac{\check{\epsilon}_{cj}}{d_j} \quad (31)$$

where $Q_{\hat{\mathbf{b}} \hat{\mathbf{z}}_c} \triangleq Q_{\hat{\mathbf{b}} \hat{\mathbf{z}}} L^{-T}$ and where $Q_{\hat{\mathbf{b}} \hat{\mathbf{z}}_c}^j$ denotes the j th column of $Q_{\hat{\mathbf{b}} \hat{\mathbf{z}}_c}$. Rewriting $\check{\mathbf{b}}$ in this way reveals that each element of the sequentially-constrained ambiguity residual $\check{\epsilon}_c$ makes a separate correction to $\hat{\mathbf{b}}$. To obtain a partially-fixed baseline, one simply truncates the summation. Thus, the

baselined constrained by only the first i ambiguities, denoted $\check{\mathbf{b}}_i$, is calculated as

$$\check{\mathbf{b}}_i = \hat{\mathbf{b}} - \sum_{j=1}^i Q_{\hat{\mathbf{b}} \check{\mathbf{z}}_c}^j \frac{\check{\epsilon}_{c(j)}}{d_j} \quad (32)$$

Its covariance $Q_{\check{\mathbf{b}}_i} \triangleq \text{cov}(\check{\mathbf{b}}_i | \check{\mathbf{z}}_{1:i} = \mathbf{z}_{1:i})$, assuming all fixed ambiguities are correct and i is chosen *a priori*, can be derived from (15). Note that $Q_{\check{\mathbf{b}}_i}$ is not the unconditional variance of $\check{\mathbf{b}}_i$ since $\check{\mathbf{z}}_{1:i}$ is a random variable with its own distribution. However, $\text{cov}(\check{\mathbf{b}}_i)$ approaches $Q_{\check{\mathbf{b}}_i}$ as the probability of success approaches one.

$$Q_{\check{\mathbf{b}}_i} = Q_{\hat{\mathbf{b}}} - \sum_{j=1}^i \frac{1}{d_j} Q_{\hat{\mathbf{b}} \check{\mathbf{z}}_c}^j \left(Q_{\hat{\mathbf{b}} \check{\mathbf{z}}_c}^j \right)^T \quad (33)$$

For high-integrity positioning, the probability distribution of the baseline vector is of great importance. It can be shown that the float baseline $\hat{\mathbf{b}} \sim \mathcal{N}(\mathbf{b}, Q_{\hat{\mathbf{b}}})$. On the other hand, the fixed IB baseline from (14) is distributed as an infinite sum of Gaussians, though, like $\hat{\mathbf{b}}$, it is unbiased [8].

Analysis of the baseline resulting from GIAB is complicated by the effects of data-driven partial fixing. If, for some reason, one decides *a priori* to fix only i ambiguities (e.g., based on the strength of the model), then, given that all fixed ambiguities are fixed correctly, $\check{\mathbf{b}}_i$ has a simple distribution:

$$\check{\mathbf{b}}_i | (\check{\mathbf{z}}_{1:i} = \mathbf{z}_{1:i}) \sim \mathcal{N}(\mathbf{b}, Q_{\check{\mathbf{b}}_i}), \quad i \in \{1, \dots, m\}$$

One might expect the same distribution to apply for GIAB when $q = i < m$. However, there is key difference between these two cases: $q = i < m$ implies that GIAB has rejected fixing the $(i + 1)$ th ambiguity. The data-driven (*a posteriori*) decision to reject yields a different baseline distribution than that of *a priori* partial fixing:

$$\check{\mathbf{b}}_i | (\check{\mathbf{z}}_{1:i} = \mathbf{z}_{1:i}, q = i < m) \approx \mathcal{N}(\mathbf{b}, Q_{\check{\mathbf{b}}_i})$$

To understand why, recall that $q = i < m$ implies GIAB rejected fixing the $(i + 1)$ th ambiguity upon finding that $|\check{\epsilon}_{c(i+1)}| \geq \beta_{(i+1)}/2$, as fixing it would violate $P_F < \bar{P}_F$. Even so, the most likely fix for the $(i + 1)$ th ambiguity, given $\check{\epsilon}_{c(i+1)}$ and given that $\check{\mathbf{z}}_{1:i} = \mathbf{z}_{1:i}$, is the same one that would have been produced by integer bootstrapping, which GIAB outputs in $\check{\mathbf{z}}_{i+1}$. The next most likely fix and its associated conditional ambiguity residual are

$$\check{\mathbf{z}}_{i+1, \text{alt}} = \check{\mathbf{z}}_{i+1} + \text{sgn}(\check{\epsilon}_{c(i+1)}) \quad (34a)$$

$$\check{\epsilon}_{c(i+1), \text{alt}} = \check{\epsilon}_{c(i+1)} - \text{sgn}(\check{\epsilon}_{c(i+1)}) \quad (34b)$$

Equation (32) indicates that if the $(i + 1)$ th integer were to be fixed, the adjustments to $\check{\mathbf{b}}_i$ in the most likely and alternate cases would be

$$\check{\mathbf{b}}_{i+1} - \check{\mathbf{b}}_i = -Q_{\hat{\mathbf{b}} \check{\mathbf{z}}_c}^{(i+1)} \frac{\check{\epsilon}_{c(i+1)}}{d_{i+1}} \quad (35a)$$

$$\check{\mathbf{b}}_{i+1, \text{alt}} - \check{\mathbf{b}}_i = -Q_{\hat{\mathbf{b}} \check{\mathbf{z}}_c}^{(i+1)} \frac{\check{\epsilon}_{c(i+1), \text{alt}}}{d_{i+1}} \quad (35b)$$

It is shown in [24] that either $\check{\mathbf{b}}_{i+1}$ or $\check{\mathbf{b}}_{i+1, \text{alt}}$ is unbiased when conditioned on $\check{\epsilon}_{c(i+1)}$ and $\check{\mathbf{z}}_{i+1} \in \{\check{\mathbf{z}}_{i+1}, \check{\mathbf{z}}_{i+1, \text{alt}}\}$, and that $P(\mathbf{z}_{i+1} \in \{\check{\mathbf{z}}_{i+1}, \check{\mathbf{z}}_{i+1, \text{alt}}\} | \check{\epsilon}_{c(i+1)}, q = i) > 1 - \bar{P}_F$. It

follows that, having examined $\check{\epsilon}_{c(i+1)}$, but having rejected the correction it offers, and the correction $\check{\epsilon}_{c(i+1), \text{alt}}$ offers, ($\check{\mathbf{b}}_i | \check{\epsilon}_{c(i+1)} = \epsilon, q = i$) is biased for any $\epsilon \neq 0$. Further, because the rejection region does not contain the origin – otherwise the fix would be accepted – averaging over the support of $\check{\epsilon}_{c(i+1)} | q = i$ implies that the distribution of ($\check{\mathbf{b}}_i | \check{\mathbf{z}}_{1:i} = \mathbf{z}_{1:i}, q = i < m$) will not have an unbiased mode. Therefore, for data-driven partial fixing, it is wrong—and *potentially hazardous*—to assume the resulting constrained baseline estimate is unbiased and unimodal. For a complete discussion on the integrity implications of partial ambiguity resolution, and for development of the *a priori* and *a posteriori* partially-fixed baseline distributions, see [24].

V. VALIDATION VIA MONTE CARLO SIMULATION

To validate the GIAB event probabilities P_F , P_U , and $P_{S_i}, \forall i \in \{1, \dots, m\}$, extensive Monte Carlo simulations were performed on float solution models with varying measurement error but the same satellite geometry. For each model, the simulation was initialized by computing the decorrelating Z-transform and using P_E -weighting to set the integer aperture parameters. Then a large sample was drawn from the distribution described by (2) to generate the float solution errors, the float baseline, and float ambiguities. The float ambiguities were then Z-transformed and the GIAB algorithm was applied to the transformed float ambiguity solution. Finally, the outputs were logged, including the number of correctly fixed samples, tabulated by q , the number of incorrectly fixed samples, tabulated by the first errant ambiguity, and the partially-fixed baseline error, tabulated by q .

The sample size for each simulation was chosen to ensure that a statistically significant number of failures occurred or a significant number of solutions was available for each value of q . This paper's theoretical event probabilities were then compared to the simulated results. To examine the goodness of fit between theory and simulation, the differences between predicted and simulated probabilities were calculated, normalized by the expected standard deviation in the measured rate.

Several models were simulated to illustrate a range of failure rates and fixing probabilities. Only small models with 7 ambiguities are presented in full detail, but similar results were obtained for $m \in \{14, 21, 28\}$. In the following tables, \mathcal{E} is an event, whether F , U , or S_i for $i \in \{1, \dots, m\}$, $P_{\mathcal{E}}$ is the predicted event probability, $\hat{P}_{\mathcal{E}}$ is the event probability as measured from the Monte Carlo simulation, and $k_{P_{\mathcal{E}}}$ is the normalized difference between the predicted and estimated event probabilities. The predicted probability of failure was computed using the bound on P_{Ei} given in (26). The difference is normalized by the standard deviation of the Beta distribution, $\beta(n_{MC} P_{\mathcal{E}}, n_{MC}(1 - P_{\mathcal{E}}))$, which is the posterior distribution of $P_{\mathcal{E}}$ given the Monte Carlo results. Thus,

$$k_{P_{\mathcal{E}}} = \frac{\hat{P}_{\mathcal{E}} - P_{\mathcal{E}}}{\sqrt{\frac{P_{\mathcal{E}}(1 - P_{\mathcal{E}})}{n_{MC}}}} \quad (36)$$

The value of $k_{P_{\mathcal{E}}}$ is interpreted as follows: if $|k_{P_{\mathcal{E}}}| < N$, then the predicted and measured probabilities differ by no more than N standard deviations.

Table II shows the simulation results for $n_{MC} = 4 \times 10^8$ Monte Carlo samples from a float distribution with a bootstrap probability of correct fix $P_{CF,B} = 1 - 2 \times 10^{-5}$ for $\bar{P}_F = 10^{-8}$. This strong model was chosen to validate the event probabilities when partial fixing is rarely needed. Table III

TABLE II
PREDICTED VS SIMULATED EVENT PROBABILITIES FOR A STRONG MODEL

\mathcal{E}	$P_{\mathcal{E}}$	$\hat{P}_{\mathcal{E}}$	$k_{P_{\mathcal{E}}}$
F	10^{-8}	$5e-9$	1.0000
U	0.0007217	0.0007204	1.0098
S_1	0.0004399	0.0004396	0.2180
S_2	0.0005133	0.0005131	0.1440
S_3	0.0011997	0.0012005	-0.4574
S_4	0.0009000	0.0009023	-1.4966
S_5	0.0018919	0.0018902	0.7913
S_6	0.0003955	0.0003956	0.0896
S_7	0.9939380	0.9939380	-0.0864

shows the simulation results for $n_{MC} = 2.2 \times 10^7$ Monte Carlo samples from a float distribution with a bootstrap probability of correct fix $P_{CF,B} = 0.988$ and $\bar{P}_F = 10^{-5}$. This weak model was chosen to validate the event probabilities when partial fixing must be employed frequently.

TABLE III
PREDICTED VS SIMULATED EVENT PROBABILITIES FOR A WEAK MODEL

\mathcal{E}	$P_{\mathcal{E}}$	$\hat{P}_{\mathcal{E}}$	$k_{P_{\mathcal{E}}}$
F	0.00001	0.0000101	-0.2673
U	0.13872	0.138628	1.1858
S_1	0.09308	0.093210	-2.2452
S_2	0.08423	0.084117	1.9596
S_3	0.09987	0.099910	-0.8364
S_4	0.07162	0.071578	0.6782
S_5	0.08010	0.080070	0.2955
S_6	0.03362	0.033647	-0.7922
S_7	0.39878	0.398801	-0.2348

As can be seen in Tables II and III, both the strong and weak model predictions match the simulation results well.

VI. COMPARISON AGAINST EXISTING IA METHODS

To demonstrate the improved performance of the GIAB aperture sizing algorithm, GIAB was compared with existing IA methods within Monte Carlo simulations for $m \in \{2, 7\}$. For the $m = 7$ simulation, a single representative satellite geometry was used with the measurement covariance scaled in the same way as described in section V to give a weak model that would test GIAB in the least favorable circumstance for comparison with the optimal IA method. IAB and GIAB compare similarly to the $m = 2$ case, so results are not tabulated for IAB for compactness. Table IV shows the results for GIAB. Note the greatest benefit of GIAB is in partial ambiguity resolution: whereas optimal IA correctly resolves the full set of ambiguities less than 84.2% of the time, GIAB correctly fixes some ambiguities almost 95% of the time, and more than half the ambiguities over 82% of time. Examination of the joint probabilities illustrates that the majority of fixes

TABLE IV
JOINT PROBABILITY MASS FUNCTION OF GIAB (ROWS) AND OPTIMAL IA (COLUMNS) FIXING DECISION FOR WEAK $m = 7$ MODEL

	S_{opt}	U_{opt}	F_{opt}	Marginal
$S_{7,GIAB}$	0.6992	0.0064	0	0.7056
$S_{6,GIAB}$	0.0009	0.0231	0	0.0239
$S_{5,GIAB}$	0.0279	0.0253	5E-6	0.0532
$S_{4,GIAB}$	0.0051	0.0360	7.5E-6	0.0411
$S_{3,GIAB}$	0.0170	0.0340	0	0.0510
$S_{2,GIAB}$	0.0227	0.0144	0	0.0370
$S_{1,GIAB}$	0.0286	0.0089	0	0.0374
U_{GIAB}	0.0403	0.0103	5.8E-5	0.0506
F_{GIAB}	0	5E-5	2.8E-5	7.8E-5
Marginal	0.8415	0.1584	9.8E-5	1

rejected by the optimal method are partially fixed by the GIAB algorithm.

For the $m = 2$ simulation, the same set of 10^6 float ambiguity samples was processed using the optimal IA method, the ellipsoidal IA method, IAB, and GIAB. The results are visualized by a scatter plot of the float ambiguities in Fig. 3. Each point is shaded according the results of the optimal IA method: dark gray points were correctly fixed, light gray points were left floating, and large, red points were fixed incorrectly.

The apertures of the ellipsoidal, IAB, GIAB, and optimal methods are plotted over the scatter plot to illustrate the comparative probability of successfully fixing all integers for $\bar{P}_F = 10^{-5}$. The threshold for the optimal method was set using a larger Monte Carlo simulation of 10^7 samples such that exactly $n_{MC} \times \bar{P}_F - 1 = 99$ failures occur. This threshold was then used to determine the outcome of the optimal IA method for the smaller simulations. For visualization, the optimal aperture region was approximated by solving for its location along a polar grid with spacings of 0.1° .

It is visually apparent that both IAB, which applies a single threshold, and GIAB, which applies two different risk-allocated thresholds, are superior to ellipsoidal IA for the model considered. There is also a visually perceptible improvement from IAB to GIAB; the exact improvement is quantified in Tables V and VI. The similarity between the GIAB and optimal apertures is clear. It is not visible, but is important to note that the GIAB aperture is slightly wider than the optimal aperture in the region of highest density. Since the optimal threshold must be set by Monte Carlo simulation, it is possible that it will perform worse than GIAB in practice though it is optimal in theory. This is the case for the results shown in Table VI.

Table V compares the ambiguity resolution performance of IAB with a single aperture threshold to that of the optimal IA estimator. This example was for a relatively lax incorrect fix risk of $\bar{P}_F = 10^{-5}$, so the performance is quite similar: the percent of samples where IAB rejects a fix that the optimal method correctly accepts is only 0.26%. Compare these results to Table VI, in which the percent of samples where GIAB rejects a fix that the optimal method correctly accepts is significantly lower, 0.0074%. Moreover, GIAB correctly accepts more fixes that the optimal method rejects. The main advantage of GIAB over optimal IA is that GIAB allows

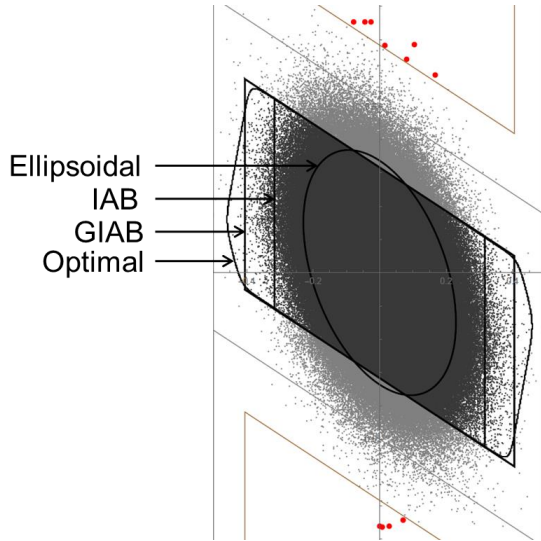


Fig. 3. Comparison of the integer aperture acceptance regions for integer aperture bootstrapping (IAB), ellipsoidal IA, GIAB, and optimal IA. All apertures allow the same expected number of incorrect fixes, but yield different rates of accepting the correct fix. Listed in ascending order of success are the ellipsoidal, IAB, GIAB, and optimal IA acceptance regions. There is a significant improvement from IAB to GIAB as many more correct fixes are admitted. The optimal IA decisions only differ from the GIAB decisions in a small fraction of cases. The scatter plot are color coded by optimal IA event: dark gray for success, light gray for undecided, and large red for failure.

partial ambiguity resolution. GIAB correctly partially fixes 4.1% of all samples, all of which are rejected by the optimal method.

TABLE V
JOINT PROBABILITY MASS FUNCTION OF IAB (ROWS) AND OPTIMAL IA (COLUMNS) FIXING DECISION FOR $m = 2$ MODEL

	S_{opt}	U_{opt}	F_{opt}	Marginal
S_{IAB}	0.954108	0.001876	0	0.955984
U_{IAB}	0.002623	0.041382	0	0.044005
F_{IAB}	0	0	0.000011	0.000011
Marginal	0.956731	0.043258	0.000011	1

TABLE VI
JOINT PROBABILITY MASS FUNCTION OF GIAB (ROWS) AND OPTIMAL IA (COLUMNS) FIXING DECISION FOR $m = 2$ MODEL

	S_{opt}	U_{opt}	F_{opt}	Marginal
S_2	0.956657	0.001791	0	0.958448
S_1	0	0.041416	0	0.041416
U_{GIAB}	0.000074	0.000051	0	0.000125
F_{GIAB}	0	0	0.000011	0.000011
Marginal	0.956731	0.043258	0.000011	1

VII. CONCLUSIONS

A new data-driven CDGNSS partial ambiguity resolution and validation algorithm has been developed analytically and validated with Monte Carlo simulation. The new algorithm has advantages over the state-of-the-art in that (1) data-driven

methods offer improved availability of integrity over model-driven methods, (2) the integrity risk due to incorrect fixing is precisely controlled analytically as compared to functional approximation methods used with the ratio test and similar integer aperture methods, and (3) it provides superior probability of success when compared to IAB or ellipsoidal IA and approaches that of optimal IA. In simulation testing, the new algorithm was shown to provide superior performance to the current state-of-the-art methods for a range of measurement models. GIAB's partial fixing, together with its analytical connection between the allowable failure rate and its validation thresholds, make GIAB attractive for safety-of-life systems in challenging environments.

ACKNOWLEDGMENTS

The authors gratefully acknowledge the Naval Air Systems Command (NAVAIR) of the U.S. Navy for supporting this research. However, the opinions discussed here are those of the authors and do not necessarily represent those of the U.S. Navy or any other affiliated agencies. Todd Humphreys's work has been supported by the National Science Foundation under Grant No. 1454474 and by the Data-supported Transportation Operations and Planning Center (DSTOP), a Tier 1 USDOT University Transportation Center.

APPENDIX A

Adopting the notation from Section II-A, the sequentially-constrained float ambiguity vector, \hat{z}_c , is defined such that its i th element is $\hat{z}_{ci} = \hat{z}_{i|I}$. Each \hat{z}_{ci} is computed as

$$\hat{z}_{ci} = \begin{cases} \hat{z}_i & i = 1 \\ \hat{z}_i - \sum_{k=1}^{i-1} l_{ik}(\hat{z}_{ck} - \hat{z}_k) & i \in \{2, \dots, m\} \end{cases} \quad (37)$$

where l_{ik} is the i, k entry in the matrix L . Because L is unit lower triangular, (37) can be expressed in vector form as

$$\hat{z}_c = \hat{z} - (L - I)(\hat{z}_c - \hat{z}) \quad (38)$$

Rearranging and collecting terms in L yields

$$\check{\epsilon} \triangleq \hat{z} - \hat{z} = L(\hat{z}_c - \hat{z}) \quad (39)$$

Multiplication by L^{-1} produces

$$\check{\epsilon}_c \triangleq L^{-1}\check{\epsilon} = \hat{z}_c - \hat{z} \quad (40)$$

REFERENCES

- [1] M. Joerger and M. Spenko, "Towards navigation safety for autonomous cars," *Inside GNSS*, vol. Nov/Dec, pp. 40–49, 2017.
- [2] S. Wu, S. R. Peck, R. M. Fries, and G. A. McGraw, "Geometry extra-redundant almost fixed solutions: A high integrity approach for carrier phase ambiguity resolution for high accuracy relative navigation," in *ionplans*, 2008, pp. 568–582.
- [3] S. Khanafseh and B. Pervan, "A new approach for calculating position domain integrity risk for cycle resolution in carrier phase navigation systems," in *Proceedings of the IEEE/ION PLANS Meeting*, May 2008, pp. 583–591.
- [4] —, "New approach for calculating position domain integrity risk for cycle resolution in carrier phase navigation systems," *IEEE Transactions on Aerospace and Electronic Systems*, vol. 46, no. 1, pp. 296–307, 2010.
- [5] S. Khanafseh, M. Joerger, and B. Pervan, "Integrity risk of cycle resolution in the presence of bounded faults," in *Proceedings of the IEEE/ION PLANS Meeting*, April 2012, pp. 664–672.

- [6] S. Khanafseh and B. Pervan, "Detection and mitigation of reference receiver faults in differential carrier phase navigation systems," *IEEE Transactions on Aerospace and Electronic Systems*, vol. 47, no. 4, pp. 2391–2404, Oct. 2011.
- [7] P. Teunissen, "Integer aperture GNSS ambiguity resolution," *Artificial Satellites*, vol. 38, no. 3, pp. 79–88, 2003.
- [8] P. J. G. Teunissen, "The probability distribution of the ambiguity bootstrapped gnss baseline," *Journal of Geodesy*, vol. 75, no. 5-6, pp. 267–275, 2001. [Online]. Available: <http://dx.doi.org/10.1007/s001900100172>
- [9] P. Teunissen, P. De Jonge, and C. Tiberius, "The least-squares ambiguity decorrelation adjustment: its performance on short GPS baselines and short observation spans," *Journal of geodesy*, vol. 71, no. 10, pp. 589–602, 1997.
- [10] P. Teunissen, "Integer aperture bootstrapping: a new GNSS ambiguity estimator with controllable fail-rate," *Journal of Geodesy*, vol. 79, no. 6-7, pp. 389–397, 2005. [Online]. Available: <http://dx.doi.org/10.1007/s00190-005-0481-y>
- [11] —, "A carrier phase ambiguity estimator with easy-to-evaluate fail-rate," *Artificial Satellites*, vol. 38, no. 3, pp. 89–96, 2003.
- [12] H.-J. Euler and B. Schaffrin, *On a Measure for the Discernibility between Different Ambiguity Solutions in the Static-Kinematic GPS-Mode*. New York, NY: Springer New York, 1991, pp. 285–295. [Online]. Available: https://doi.org/10.1007/978-1-4612-3102-8_26
- [13] S. Verhagen and P. Teunissen, "The ratio test for future gnss ambiguity resolution," *GPS Solutions*, vol. 17, no. 4, pp. 535–548, 2013. [Online]. Available: <http://dx.doi.org/10.1007/s10291-012-0299-z>
- [14] C. Tiberius and P. J. D. Jonge, "Fast positioning using the lambda-method," in *Proceedings of the 4th International Symposium on Differential Satellite Navigation Systems DSNS'95*, 1995, pp. 24–28.
- [15] J. Zhang, M. Wu, T. Li, and K. Zhang, "Integer aperture ambiguity resolution based on difference test," *Journal of Geodesy*, vol. 89, no. 7, pp. 667–683, 2015. [Online]. Available: <http://dx.doi.org/10.1007/s00190-015-0806-4>
- [16] P. Teunissen, "GNSS ambiguity resolution with optimally controlled failure-rate," *Artificial Satellites*, vol. 40, no. 4, pp. 219–227, 2005.
- [17] S. Verhagen and P. J. Teunissen, "New global navigation satellite system ambiguity resolution method compared to existing approaches," *Journal of Guidance, Control, and Dynamics*, vol. 29, no. 4, pp. 981–991, 2006.
- [18] P. Teunissen and S. Verhagen, "The GNSS ambiguity ratio-test revisited: a better way of using it," *Survey Review*, vol. 41, no. 312, pp. 138–151, 2009. [Online]. Available: <http://dx.doi.org/10.1179/003962609X390058>
- [19] L. Wang and S. Verhagen, "A new ambiguity acceptance test threshold determination method with controllable failure rate," *Journal of Geodesy*, vol. 89, no. 4, pp. 361–375, 2015. [Online]. Available: <http://dx.doi.org/10.1007/s00190-014-0780-2>
- [20] A. Brack, "On reliable data-driven partial GNSS ambiguity resolution," *GPS Solutions*, vol. 19, no. 3, pp. 411–422, 2015. [Online]. Available: <http://dx.doi.org/10.1007/s10291-014-0401-9>
- [21] P. J. G. Teunissen, "GNSS ambiguity resolution with optimally controlled failure-rate," *Artificial Satellites*, vol. 40, pp. 219–227, 2005.
- [22] A. Brack and C. Gunther, "Generalized integer aperture estimation for partial GNSS ambiguity fixing," *Journal of Geodesy*, vol. 88, no. 5, pp. 479–490, 2014. [Online]. Available: <http://dx.doi.org/10.1007/s00190-014-0699-7>
- [23] G. N. Green, M. King, and T. E. Humphreys, "Data-driven generalized integer aperture bootstrapping for real-time high integrity applications," in *Proceedings of the IEEE/ION PLANS Meeting*, Savannah, GA, 2016.
- [24] G. N. Green and T. E. Humphreys, "Position domain integrity analysis for generalized integer aperture bootstrapping," *IEEE Transactions on Aerospace and Electronic Systems*, 2017, submitted for review. [Online]. Available: <http://goo.gl/qgKu9W>
- [25] P. J. Teunissen, "The least-squares ambiguity decorrelation adjustment: a method for fast GPS integer ambiguity estimation," *Journal of Geodesy*, vol. 70, no. 1-2, pp. 65–82, 1995.
- [26] M. Psiaki and S. Mohiuddin, "Global positioning system integer ambiguity resolution using factorized least-squares techniques," *Journal of Guidance, Control, and Dynamics*, vol. 30, no. 2, pp. 346–356, March-April 2007.
- [27] Y. Bar-Shalom, X. R. Li, and T. Kirubarajan, *Estimation with Applications to Tracking and Navigation*. New York: John Wiley and Sons, 2001.
- [28] P. Teunissen, "Success probability of integer GPS ambiguity rounding and bootstrapping," *Journal of Geodesy*, vol. 72, no. 10, pp. 606–612, 1998.